26th ABCM International Congress of Mechanical Engineering
November 22-26, 2021. Florianópolis, SC, Brazil

EULERIAN-EULERIAN CFD SIMULATION OF BIOMASS DEVOLATILIZATION IN FLUIDIZED BED REACTOR FOR GASIFICATION

Vitor Alberto Lemes Monteiro
Maurício Guilherme Alves dos Reis
Universidade Federal de Uberlândia, Faculdade de Engenharia Mecânica, Av. João Naves de Ávila, 2121, 38408-100, Uberlândia-MG.
vitoralbertolemes@hotmail.com, mauricioalvesreis@gmail.com

Luciano Reis Infiesta
Carbogás Energia, Avenida Guaraciaba, 659, 09370-840, Mauá-SP.
luciano@carbogas.com.br

Solidônio Rodrigues de Carvalho
Universidade Federal de Uberlândia, Faculdade de Engenharia Mecânica, Av. João Naves de Ávila, 2121, 38408-100, Uberlândia-MG.
solidonio@ufu.br

Abstract. *The present work is related to a municipal refuse-derived fuel gasification system with a semi-industrial fluidized bed reactor. Computational fluid dynamic modeling was implemented using the opensource software OpenFOAM v8 to simulate the biomass devolatilization of pyrolysis process in fluidized bed system. The objective of this work was to develop a model to simulate a simplified 2D reactor, able to provide consistent results of the biomass chemical processes and subprocesses of gasification. For this paper, the focus was the devolatilization reaction, due to its complexity related to biomass conversion into solid and gaseous phases. Once the homogeneous and others heterogeneous reactions were not implemented yet, it was not possible to establish a quantitatively comparison of the produced syngas composition with literature works. The Eulerian-Eulerian approach was employed to handle a three-phase system composed by silica sand and biomass particles into an air medium. The most advantage of such approach is the lower computational requirements when simulating dense particle reacting system. Mass and energy source terms was attached to mass, species and momentum balance equations to represent the chemical process of the devolatilization. The biomass consumption and conversion from the solid phase to gaseous products was modeled through Arrhenius law of devolatilization rate. Experimental data of pine wood biomass pyrolysis was used in this occasion to the simulation model. All thermophysical properties was acquired by Sutherland's Law and JANAF Thermochemical Tables. The results shows qualitatively consistent progression of devolatilization process in terms of biomass solid phase transformations into char and syngas. To reach the semi-industrial scale simulation modeling, further work consists of (i) implement the remaining heterogeneous reactions of carbon conversion and gasification homogeneous reactions, (ii) add the ash and reacting limestone solid phases and (iii) expand the reactor mesh domain to the real dimensions of the semi-industrial gasification plant.*

Keywords: *gasification, renewable energy, municipal solid waste, refuse-derived fuel, multiphase flow.*

1. INTRODUCTION

The main difficulties on engineering research are the obtaining of relevant information of real industrial or large-scale processes. For instance, the fluidized bed processes are widely applied at the industry, in which the thermochemical waste-to-energy (WTE) techniques are combined. However, the complexity of such technologies results in long term and hard researching work to scientific community, besides funding and investments.

The Computational Fluid Dynamics (CFD) modeling is nowadays one of the mostly advanced tools for engineering simulations of such industrial processes. Among the main models for simulating fluidized bed reactors, involving different levels of accuracy and depth of modeling, the most currently studied are the Eulerian and Lagrangian approaches. Such models provide the highest level of detail for physical, chemical, thermal and fluid-dynamic phenomena (Gerber, Behrendt, and Oevermann, 2010). Furthermore, they can provide important information for analysis of industrial processes and operations.

A recent work (Gupta et al., 2021) used Lagrangian approach to simulating the gasification of rice husks in a bubbling fluidized bed. The developed model was able to demonstrate characteristics of the solid-gas flow in the bed under transient regime in addition to the formation, coalescence and rupture of bubbles along the flow.

On the other hand, the main difficulty related to the simulation of this kind of problem is the large number of equations to describe the motion of substances attached to a huge number of computational cells discretized in the geometry mesh (Loha, Chattopadhyay, and Chatterjee, 2014). For example, a CFD model was developed to simulate a lab-scale rectangular gasifier of pine wood biomass (Ku, Li, and Løvås, 2015). The reactor (0.23 m width × 1.5 m height × 0.0015 m thickness) was modeled with 40,000 sand particles of 1.5 mm of diameter and CFD cell size of 0.3×10^{-6} m. The pyrolysis, char conversion and particle shrinkage equations using the Eulerian-Lagrangian approach with Discrete Element Method (DEM) was also implemented. Despite of the small amount of CFD cells and simple geometry, it was necessary about 14 days to complete the 20 s real time simulation at their computational apparatus.

Lagrangian approaches and hybrid ones are fully useful with reacting systems, but require high computational cost (Ostermeier et al., 2019; Wan et al., 2020). Therefore, the focus of this paper was on the Eulerian based modeling. In despite of its limitations attaching chemical reactions at dense multiphase flows, it still can be implemented to simulate fluidized-bed reactors, as well demonstrated in some literature works (Askaripour, 2020; Askaripour and Dehkordi, 2019; Zhong et al., 2016).

The line of research of our group is within the scope of WTE technologies and consists of the study of a semi-industrial scale fluidized bed gasification plant for the conversion of municipal solid waste (MSW) into energy. Previously study have demonstrated a solid waste processing line (SWPL) to produce the municipal refuse-derived fuel (MRDF) biomass from MSW (Infiesta et al., 2019). Such fluidized bed gasification reactor, capable of recovering syngas from MRDF, was developed in experimental basis by our research group. The future perspective is to develop a full CFD model to reproduce such reactor process and to improve this WTE gasification technology.

The objective of this paper is to implement the devolatilization process to a computational model, evaluating the conversion of biomass solid particles into gaseous phase and char.

2. COMPUTATIONAL FLUID DYNAMICS MODEL

The computational model presented below includes only the biomass devolatilization chemical reaction, which consists of converting consumable biomass into carbon and gases, as shown in Figure 1. The other chemical processes will be implemented in future works. The pyrolysis products can include liquid products depending on the process conditions. In this work, the authors preferred to neglect the tar formation (Qi et al., 2019) at such operating temperature (670 K). Besides that, the experimental gasification semi-industrial reactor operates at 1123 K, in which there was no significant amount of liquid or tar produced during experiments (Ferreira et al., 2021).

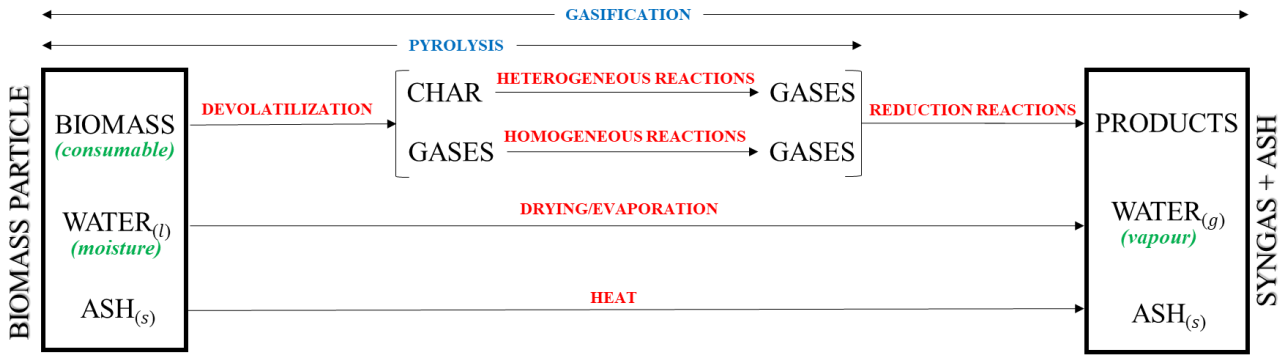

Figure 1. Pyrolysis and gasification sub-processes representation (expected for temperature about 1000 K) for computational modeling.

Pine wood biomass was used, due to the homogeneity of its composition and the availability of data in the scientific literature. The mass fractions of the products generated by pyrolysis in dry and ash-free basis, according to Qi et al. (2019), showed at. These fractions were assumed as the products of devolatilization sub-process in this work.

Table 1. Mass fraction of pyrolysis products of dry, ash-free wood (Qi et al., 2019).

Component	Mass fraction
H_2	0.106
CO	0.313
CO_2	0.146
CH_4	0.035
H_2O	0.200
Char	0.200

2.1 Governing Equations

The Eulerian-Eulerian approach solves the governing equations for each phase, in this case the gas (air) and solid (sand) phase. The sum of the volumetric particle fraction of the different phases is always unit. The governing equations for each phase were implemented as the computational methodology properly detailed by Rusche (2002) and is briefly presented below.

The mass balance equation is written as:

$$\frac{\partial}{\partial t}\alpha_k\rho_k + \frac{\partial}{\partial x_i}\alpha_k\rho_k U_k = \dot{m}_k + \dot{m}_{p\to i,k}, \tag{1}$$

The momentum equations are,

$$\frac{\partial}{\partial t}(\alpha_k\rho_k U_k) + \nabla\cdot(\alpha_k\rho_k U_k U_k) = \alpha_k\rho_k g_i + \nabla\cdot S_k + I_k, \tag{2}$$

$$S_k = \nabla\cdot(\alpha_k\tau_k) - \alpha_k\nabla p - \nabla p_k, \tag{3}$$

$$\tau_k = \mu_{eff}\frac{1}{2}\left[\nabla U_k + \nabla U_k^T\right] + \left(\lambda_k - \frac{2}{3}\mu_{eff}\right)(\nabla\cdot U_k)I, \tag{4}$$

Energy transport equation is given as,

$$\frac{\partial}{\partial t}(\alpha_k\rho_k E_k) + \nabla\cdot(\alpha_k\rho_k U_k E_k) = \alpha_k\left(\frac{\partial p}{\partial t} + U_k\cdot\nabla p\right) - \nabla\left(\alpha_k\kappa_{eff}\nabla T_k\right) + \phi + A_{sp}h(T^* - T_k) + \dot{q}_k, \tag{5}$$

The index k is symbolic for the solid or the fluid phase, e.g. the particle solid phase fraction (α) was denoted by α_p, the one of the gas continuous phases as α_g. The index i represents each of the species present at solid or gas phase. At such equations, α_k is the volume fraction, ρ_k the density and U_k the velocity of the respective phase. $\dot{m}_k$ is the mass source term and $\dot{m}_{p\to i,k}$ is the interphase mass transfer term of converted biomass particle (p) products into gas or solid phase.

The momentum equation defines S_k as the *k*-phase stress tensor, p the pressure, p_k the granular pressure when solid phase, λ_k the solid bulk viscosity and I_k is the momentum exchange term which may include drag forces, turbulent dispersion, etc.

k_{eff} e μ_{eff} represents the effective thermal conductive and viscosity, which also includes the turbulent effects.

At the energy transport equation, ϕ is the viscous dissipation and E_k the enthalpy, A_{sp} is the superficial area per volume unit of the particle phase, h is the convective coefficient and T^* is the temperature of the exchange phase and $\dot{q}_k$ the heat source term of the k-phase.

The drag model is written as a combination of the Ergun Equation (Ergun, 1952) and Wen and Yu drag model (1966). The drag factor is the drag factor for a spherical particle given by Schiller & Naumann (1935). The combination of the two drag models leads to Gidaspow's Drag Model (Gidaspow, 1994). The Gidaspow's Drag Model is recommended for dense particulate flow, typical of this type of reactor (Zhong et al., 2016).

Empirical correlation used for calculating the Nusselt's number (Ranz and Marshall, 1952) to the heat flux between phases:

$$Nu = 2 + 0.6Re^{0.5}\mathrm{Pr}^{0.33}, \tag{6}$$

$$Nu = \frac{hd_p}{\kappa}, \tag{7}$$

By these procedures, Eq. (6) can be used to calculate the convective coefficient (h) for the energy transport equation (Eq. 5). The Sutherlands's transport modeling (Sutherland, 1893) concerns evaluating dynamic viscosity (μ) in function of temperature from specific coefficient (A_s) and Sutherland Temperature (T_s) by the correlation:

$$\mu = \frac{A_S\sqrt{T}}{1+\frac{T_S}{T}}, \tag{8}$$

JANAF Thermochemical Tables (Chase, 1998) provides the coefficients of a polynomial relation to calculate the specific heat (c_p) as function of temperature (T).

The balance of mass fraction species (Y) is written as:

$$\frac{\partial}{\partial t}\left(\alpha_k\rho_k Y_{i,k}\right) + \nabla\cdot\left(\alpha_k\rho_k U_k Y_{i,k}\right) = \nabla\left(\alpha_k\rho_k \mathrm{D}_{\mathrm{eff}}\nabla Y_{i,k}\right) + \dot{m}_{p\to i,k}, \tag{9}$$

where D_{eff} is the effective mass diffusivity of i-specie and the terms $\dot{m}_{p\to i,k}$ represents the mass conversion (consumption or generation) of biomass particles into i-specie of k-phase. In this work, once the solid biomass particle phase if modeled with two species (consumable biomass and char), there is conversion of biomass into char.

The resultant simplified reaction for the release of the devolatilization products (Qi et al., 2019) is given by:

$$Biomass \to a_1H_2 + a_2H_2O + a_3CO + a_4CH_4 + a_5CO_2 + a_6Char, \tag{10}$$

where the constants a_i is defined as and the devolatilization rate is determined by first-order Arrhenius form:

$$R_{dev} = -AT^{\beta}\left(-\frac{E}{R_uT_p}\right), \tag{11}$$

where R_u is the universal gas constant and T_p the temperature of the particle. According to Qi et al. (2019), the frequency factor is set to $A = 5.0\times10^6$ s^{-1}, the activation energy is set to $E = 1.2\times10^8$ J kmol^{-1} and the temperature (T) exponent $\beta = 0$. This way, the mass conversion contributions are written in terms of the mass fraction of devolatilization products (n_i) of:

$$\dot{m}_{p\to i,k} = n_i(\alpha_p\rho_pY_{bio})R_{dev} \tag{12}$$

The Eq. (12) is used to the calculations of conversion terms of Eq. (9) and also Eq. (1), where Y_{bio} is solved by OpenFOAM v8 as equal unit.

Since the temperature is initially uniform throughout the domain, the heat of devolatilization process was negligible. It is worth mentioning that the biomass at Eq. (6) is considered on a dry and ash-free basis. The pyrolysis operation includes the drying process and others heterogeneous reactions.

For this model, the particle diameter shrinkage was not considered, in which this parameter remains constant over time. However, the consumption of biomass is numerically implemented by the reduction of mass fraction of biomass particles due to the devolatilization rate.

2.2 Configuration of bubbling fluidized bed reactor

The devolatilization process of the pyrolysis was implemented into a three-phase system, composed by silica sand particles solid phase, biomass particles solid phase and gaseous phase. The components of gaseous phase considered was H_2, CO, CO_2, CH_4, H_2O, O_2 and N_2. The biomass phase is composed of carbon and the chemically active matter from biomass (consumable biomass).

Simplified 2D geometry was set with 1.5 m of height and 0.15 m of width (Figure 2). This geometry has a pseudo 2D domain in which the software considers a small thickness to avoid numerical issues. This geometry was divided into squared cells of 0.0075 m of edge, totaling 4000 hexahedral finite volume cells to mesh grid.

The reactor was initially filled up to one third of its height with particles of sand and biomass, in a continuous medium of atmospheric air. The solid phase mass of total 0.10628 kg of biomass particles (100% consumable biomass) and 1.50750 kg of sand, besides the air medium (22% of O_2 and 78% of N_2). Some other simulation parameters are showed at Table 2 and initial conditions at Figure 2.

The time step of 0.25×10^{-3} was implemented as a constant parameter and total physical time adopted was 300 s to handle enough time for observation of significant thermal degradation of the biomass initial mass.

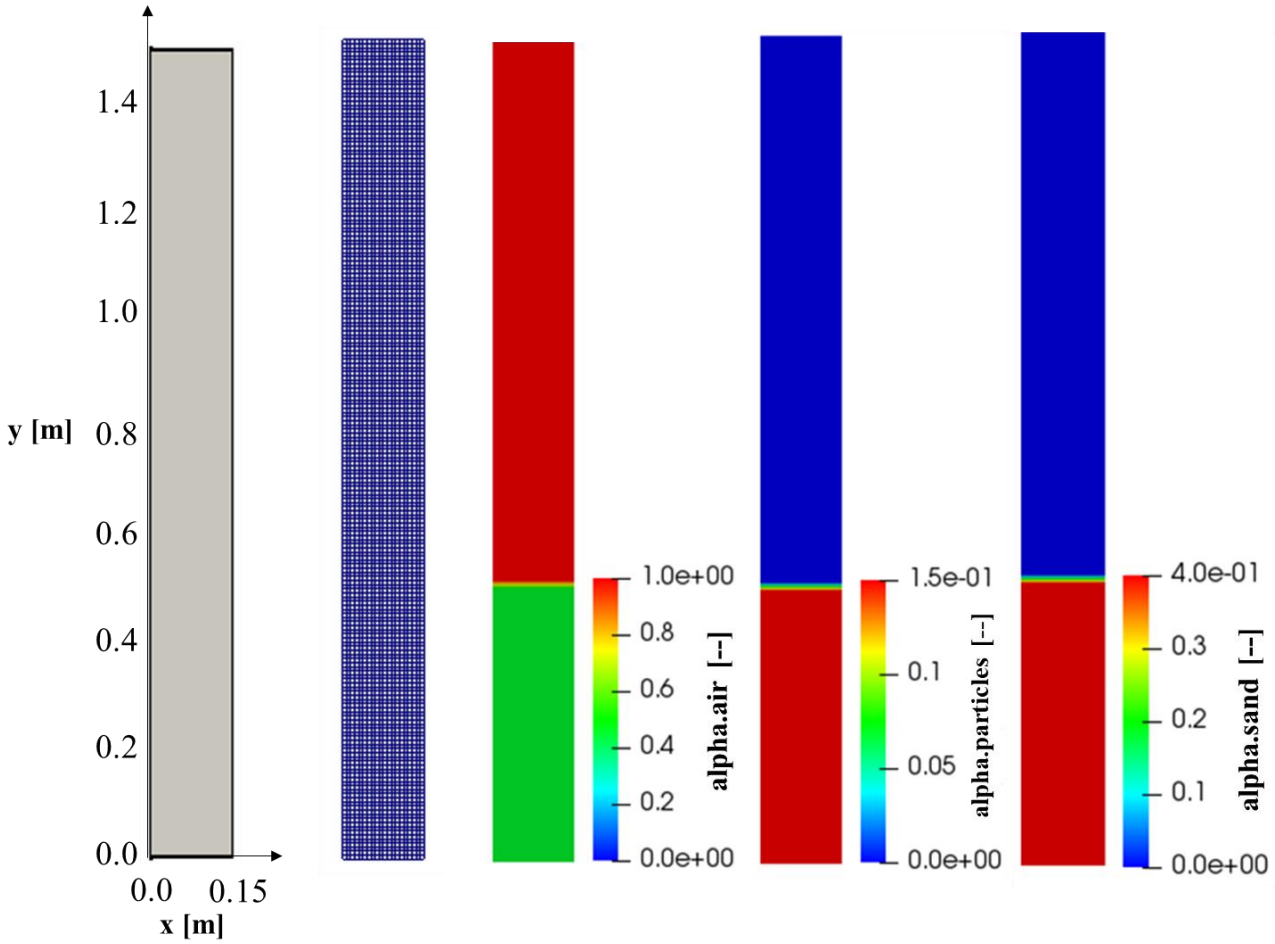

Figure 2. Representation of the geometry, mesh and initial conditions of volume particle fractions of air, particles and sand phases.

Table 2. Initial conditions and other parameters.

Parameters	**Value**
Biomass feed rate, kg/h	N/A
Biomass temperature, K	670
Biomass Particle diameter(1), m	1.5×10^{-3}
Biomass initial mass, kg	0.10628
Density of biomass(1), kg/m³	470
Density of char, kg/m³	180
Mass source term, kg/s	N/A
Energy source term, kg.m²/s³	N/A
Density of sand particles(1), kg/m³	2600
Sand particles diameter(1), m	5×10^{-4}
Temperature of air at inlet, K	670
Temperature of fluidized gas, K	670
Initial bed temperature, K	670
Operating temperature(1), K	670
Gasifier walls condition	Insulated
Interstitial inlet velocity of air, m/s	0.05
Outlet pressure, kPa	Atmospheric
Atmospheric pressure, kPa	101.325
Mesh grid square cells edge dimensions, m	0.0075

N/A – not applied, (1)Adopted same as Qi et al. (2019)

3. RESULTS AND DISCUSSION

Once the main objective was to design a functional model to handle only the devolatilization pyrolysis reaction, the following results were not compared to other literature works. When the other heterogeneous and homogeneous reactions were implemented, it would be possible to compare experiments with simulations. This way, the consistency of the model was evaluated by the mass balance and the products formation progress over time.

By the end of the simulation (300 s), the system remained with the same amount of sand, without high sand particles losses. That feature indicates a fluidized bed regime similar to smooth pattern (Kunii, D. and Levenspiel, 1991). It was not observed large amount of bubbling formation. Therefore, the inlet air velocity can be increased without major changes to the flow. Figure 3 shows the volumetric fraction of each of phases – biomass (a), silica sand (d) and air (e) – and the solid species, consumable biomass (b) and char (c). When compared to the initial configuration of the reactor (Figure 2), the biomass particles components (Figure 3 a,b,c) are moved to the upper part of the fluidized bed due to its specific mass and temperature, while the silica sand remains at the bottom (Figure 3d). The bed voidage volume fraction of the fluidized bed at the steady state is about 0.5, which is uniformly distributed to the bed height (Figure 3d). The same phenomena were observed to the char produced (Figure 3c), which occupies the interface between air phase (Figure 3e) of the reactor. The characteristic will support the occurrence heterogeneous reactions not yet implemented for the conversion of carbon into gaseous products.

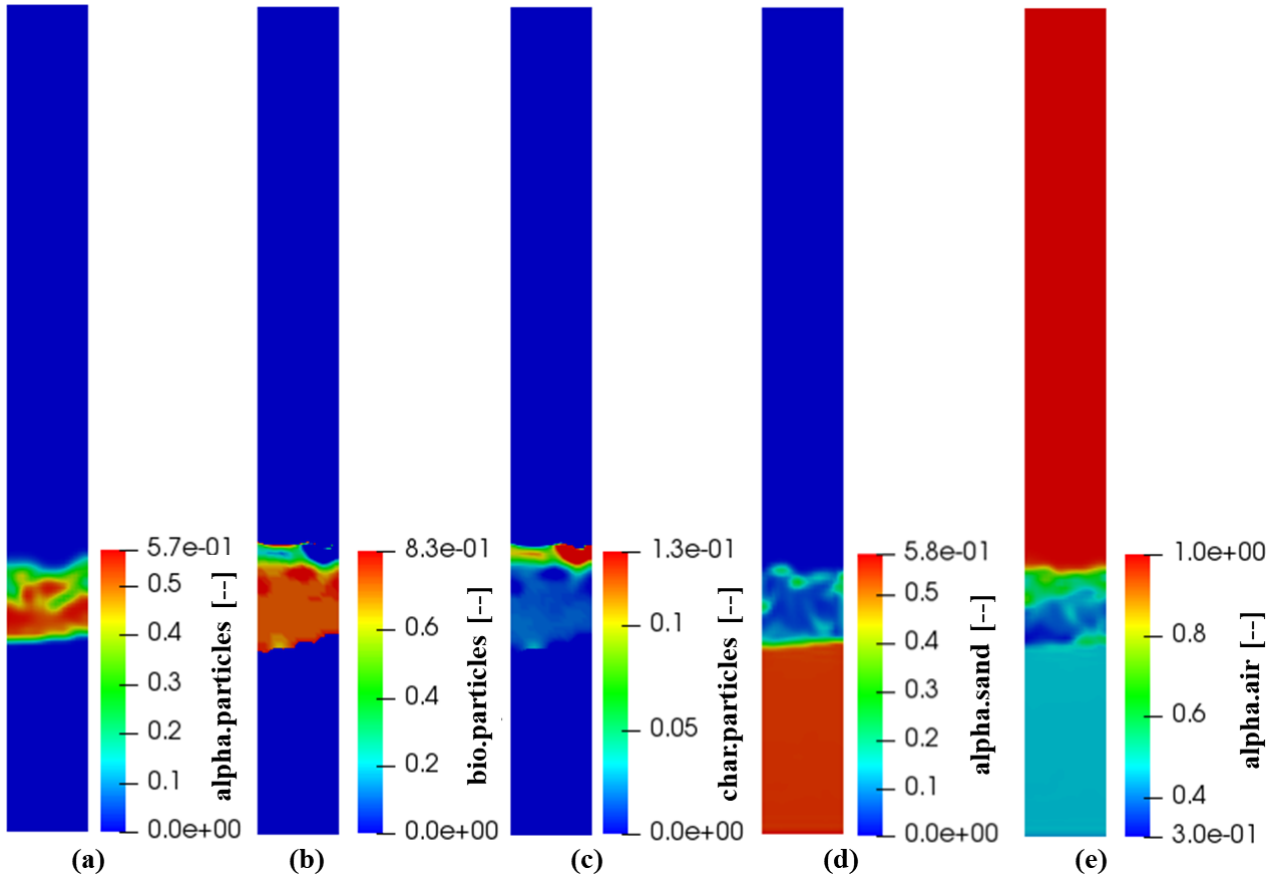

Figure 3. General aspect representation of volumetric fractions of (a) particles, (b) biomass, (c) carbon, (d) silica and (e) air.

The resulting biomass particle mass was 0.06346 kg of particles, being 83% of consumable biomass mass and 17% of produced carbon. The mass fractions composition of the synthesis gas obtained were 0.08179 kg/kg of H_2O, 0.05971 kg/kg of CO_2, 0.12799 kg/kg of CO, 0.04335 kg/kg of H_2, 0.14804 kg/kg of O_2, 0.52480 kg/kg of N_2 and 0.01431 kg/ kg of CH_4. The post-processing calculations indicates good agreement between the concentration of each species and the pre-determined proportion of the chemical reaction rates (Table 1). Consequently, carbon and gases production take place continuously according to the rates imposed in the process. Figure 4 demonstrates the volumetric fraction distribution of each of the gases produced in the biomass devolatilization process at the end of the simulation.

The steady state of the simulation is showed at Figure 5, in terms of the pressure (a), air velocity (b), particles velocity (c) and sand velocity (d). The inlet air pressure at this condition was 105,077 Pa and the maximum velocity observed was approximately 1.4 m/s of the air phase through the freeboard of the reator.

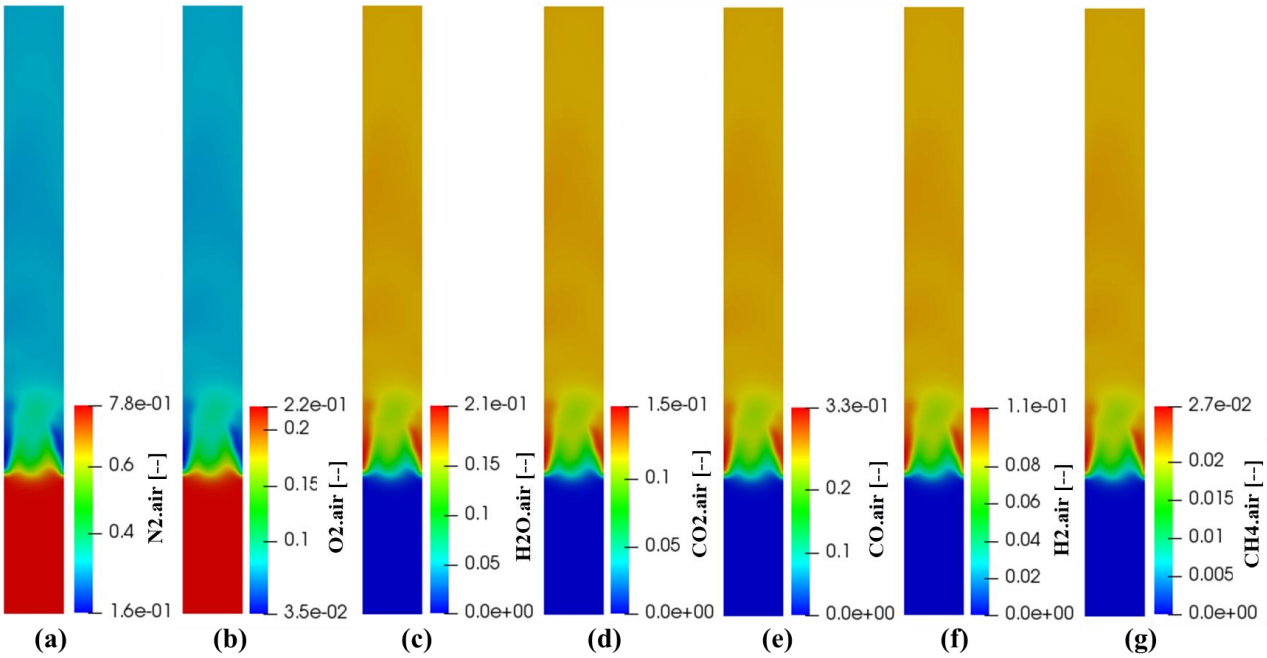

Figure 4. Representation of the volumetric fractions of produced gases species at the final stage of simulation.

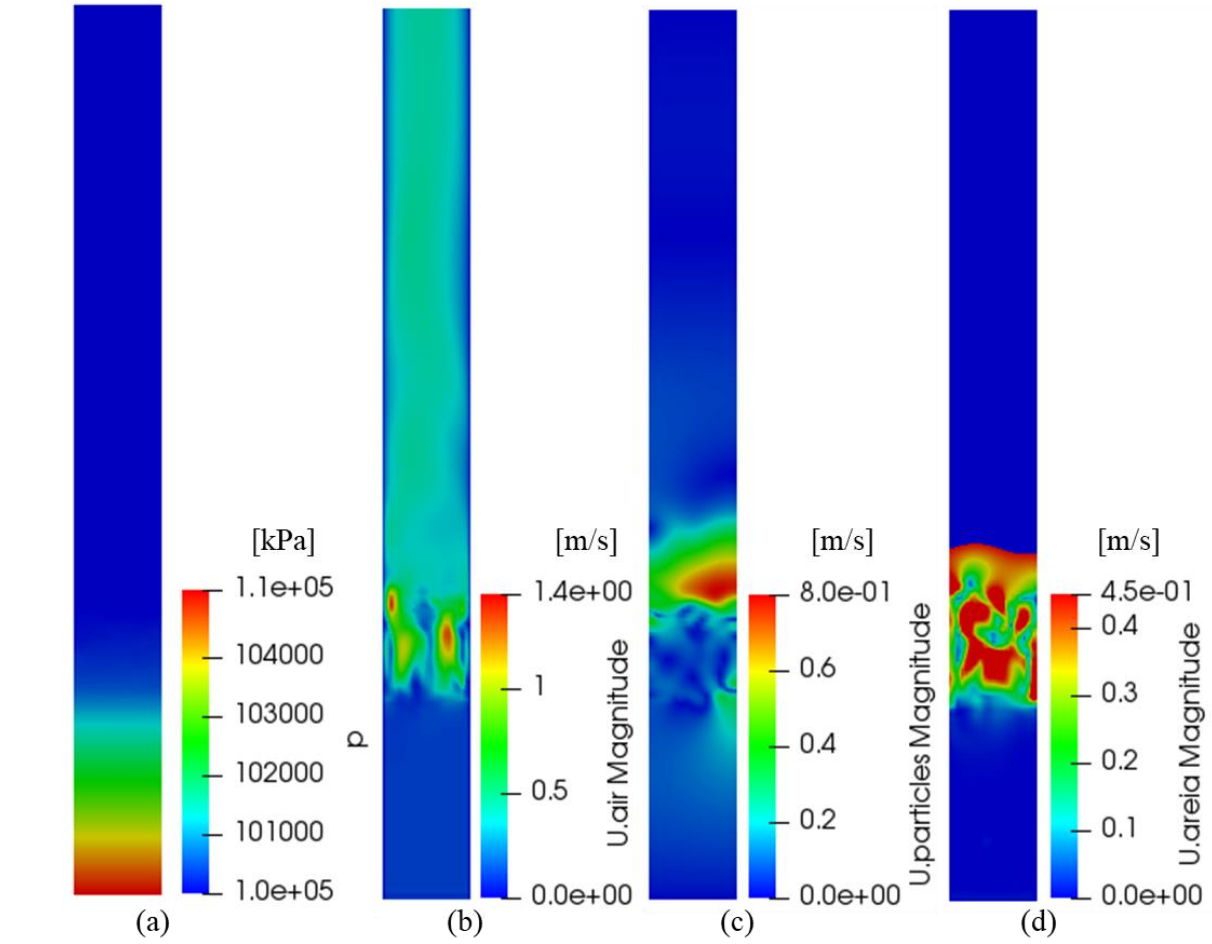

Figure 5. Representation of the (a) pressure, (b) air velocity, (c) particles velocity and (d) sand velocity at final stage of simulation.

Figure 6 shows the gas species production in function of time of simulation. At the initial times, the components of the air (O_2 and N_2), which fill the gaseous phase throughout the reactor, starts to decay and give place to the syngas' species produced by devolatilization. At the final of the simulation, all species tend to reach steady state regime.

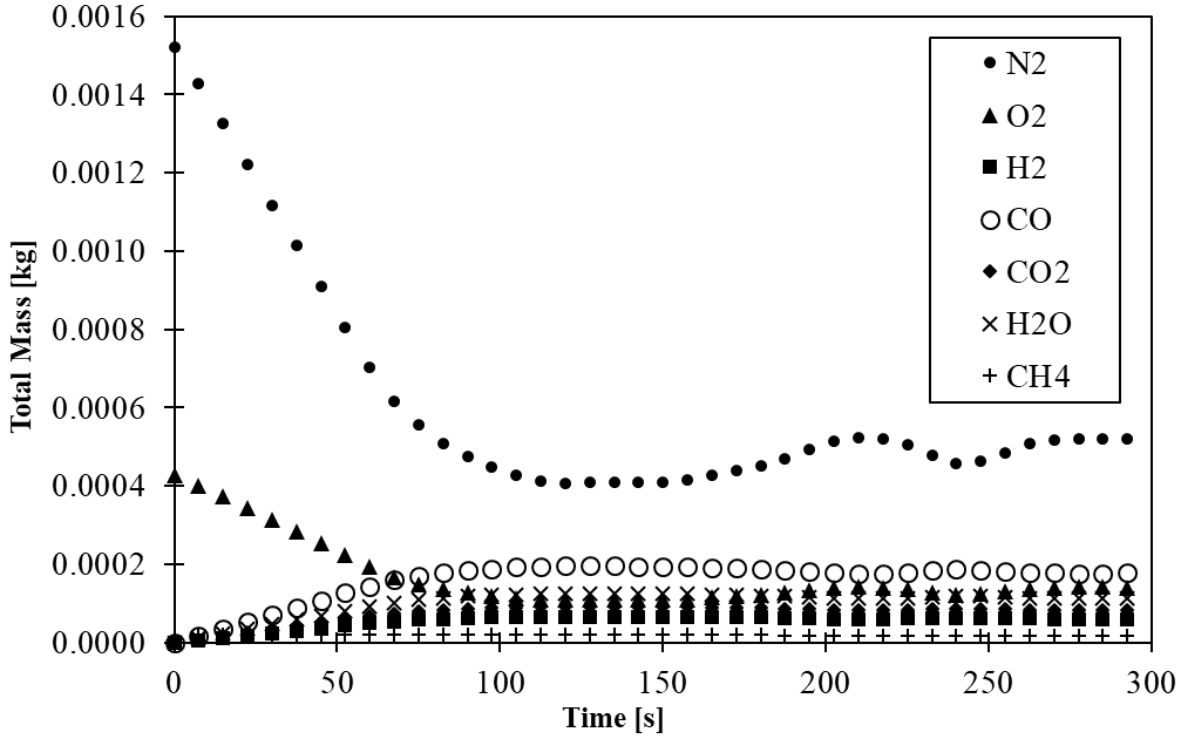

Figure 6. Produced gas species generation during the simulation.

4. CONCLUSIONS

The present work consisted of the implementation of one of the thermochemical processes of pyrolysis, called devolatilization. This is a complex process that involves the conversion of solid reactants into products in both solid and gas phase, whose modeling was carried out in order to mainly verify the mass balance and consistency of the process.

The results presented correctly demonstrate the simultaneously consumption of biomass, the production of carbon and the gases of interest in this process. Those were also useful to better comprehension of thermal degradations of biomass related to the devolatilization process.

The future perspective is to implement the other heterogeneous reactions, homogeneous reactions and combustion reactions in order to obtain a complete modeling of the biomass gasification process in a fluidized bed.

In future work, the following improvements must still be contemplated for simulation modeling on a semi-industrial scale: *(i)* implement the remaining heterogeneous carbon conversion reactions and homogeneous gasification reactions, *(ii)* add the reactive limestone solid phase to the process and *(iii)* expand the reactor mesh domain to the real semi-industrial scale design dimensions.

5. ACKNOWLEDGEMENTS

The authors are grateful for the financial support provided by Furnas Centrais Elétricas S.A., Carbogás Energia Ltda., Agência Nacional de Energia Elétrica, Coordenação de Aperfeiçoamento de Pessoal de Nível Superior (CAPES), Conselho Nacional de Desenvolvimento Científico e Tecnológico (CNPq), and Fundação de Amparo à Pesquisa do Estado de Minas Gerais (FAPEMIG).

6. REFERENCES

Askaripour, H., 2020. "CFD Modeling of Gasification Process in Tapered Fluidized Bed Gasifier". *Energy* Vol. 191, No. 1, .

Askaripour, H., and Dehkordi, A. M., 2019. "Two-Dimensional CFD Simulation of Chemical Reactions in Tapered-in and Tapered-out Fluidized Bed Reactors". *Advanced Powder Technology* Vol. 30, No. 1, pp. 136–47.

Chase, M. W., 1998. "NIST-JANAF Thermochemical Tables, 4th Ed. J. Phys. Chem. Ref. Data. 1998, Monograph 9(Part

I and Part II)". *Journal of Physical and Chemical Reference Data* Vol. Monograph, pp. Part I&II.

Ergun, S., 1952. "Fluid Flow through Packed Columns".

Ferreira, C. R. N., Infiesta, L. R., Monteiro, V. A. L., Starling, M. C. V. M., da Silva Júnior, W. M., Borges, V. L., Carvalho, S. R., and Trovó, A. G., 2021. "Gasification of Municipal Refuse-Derived Fuel as an Alternative to Waste Disposal: Process Efficiency and Thermochemical Analysis". *Process Safety and Environmental Protection* Vol. 149, No. 1, pp. 885–93.

Gerber, S., Behrendt, F., and Oevermann, M., 2010. "An Eulerian Modeling Approach of Wood Gasification in a Bubbling Fluidized Bed Reactor Using Char as Bed Material". *Fuel* Vol. 89, No. 10, pp. 2903–17.

Gidaspow, D., 1994. *Multiphase Flow and Fluidization: Continuum and Kinetic Theory Descriptions*. doi: 10.1016/C2009-0-21244-X.

Gupta, S., Choudhary, S., Kumar, S., and De, S., 2021. "Large Eddy Simulation of Biomass Gasification in a Bubbling Fluidized Bed Based on the Multiphase Particle-in-Cell Method". *Renewable Energy* Vol. 163, pp. 1455–66.

Infiesta, L. R., Ferreira, C. R. N., Trovó, A. G., Borges, V. L., and Carvalho, S. R., 2019. "Design of an Industrial Solid Waste Processing Line to Produce Refuse-Derived Fuel". *Journal of Environmental Management* Vol. 236, No. 1, pp. 715–19.

Ku, X., Li, T., and Løvås, T., 2015. "CFD-DEM Simulation of Biomass Gasification with Steam in a Fluidized Bed Reactor". *Chemical Engineering Science* Vol. 122, pp. 270–83.

Kunii, D. and Levenspiel, O., 1991. *Fluidization Engineering*. Butterworth-Heinemann Series in Chemical Engineering. doi: 10.1016/b978-0-7506-9236-6.50001-9.

Loha, C., Chattopadhyay, H., and Chatterjee, P. K., 2014. "Three Dimensional Kinetic Modeling of Fluidized Bed Biomass Gasification". *Chemical Engineering Science* Vol. 109, pp. 53–64.

Ostermeier, P., Fischer, F., Fendt, S., DeYoung, S., and Spliethoff, H., 2019. "Coarse-Grained CFD-DEM Simulation of Biomass Gasification in a Fluidized Bed Reactor". *Fuel* Vol. 255, No. 1, pp. 115790.

Qi, T., Lei, T., Yan, B., Chen, G., Li, Z., Fatehi, H., Wang, Z., and Bai, X. S., 2019. "Biomass Steam Gasification in Bubbling Fluidized Bed for Higher-H2 Syngas: CFD Simulation with Coarse Grain Model". *International Journal of Hydrogen Energy* Vol. 44, No. 13, pp. 6448–60.

Ranz, W. E., and Marshall, W. R., 1952. "Evaporation from Drops". *Chem. Eng. Progr* Vol. 48, No. 22, pp. 141–73.

Rusche, H., 2002. "Computational Dispersed Two-Phase Dynamics Flows of At Phase Fractions". No. 1, .

Schiller, L., and Naumann, Z., 1935. "A Drag Coefficient Correlation". *Z.Ver.Deutsch.Ing* Vol. 77, No. 13–14, pp. 318–20.

Sutherland, W., 1893. "The Viscosity of Gases and Molecular Force". *The London, Edinburgh, and Dublin Philosophical Magazine and Journal of Science* Vol. 36, No. 223, pp. 507–31.

Wan, Z., Yang, S., Wei, Y., Hu, J., and Wang, H., 2020. "CFD Modeling of the Flow Dynamics and Gasification in the Combustor and Gasifier of a Dual Fluidized Bed Pilot Plant". *Energy* Vol. 198, .

Wen, C. Y., and Yu, Y. H., 1966. "A Generalized Method for Predicting the Minimum Fluidization Velocity". *AIChE Journal* Vol. 12, No. 3, pp. 610–12.

Zhong, W., Yu, A., Zhou, G., Xie, J., and Zhang, H., 2016. "CFD Simulation of Dense Particulate Reaction System: Approaches, Recent Advances and Applications". *Chemical Engineering Science* Vol. 140, pp. 16–43.

7. RESPONSIBILITY NOTICE

The authors are the only responsible for the printed material included in this paper.